An organic silver complex conductive ink using both decomposition and self-reduction mechanisms in film formation

Wendong Yang[a], Changhai Wang[a, *] and Valeria Arrighi[b]

[a] Institute of Sensors, Signals and Systems, School of Engineering and Physical Sciences, Heriot-Watt University, Edinburgh, EH14 4AS, UK

[b] Institute of Chemical Sciences, School of Engineering and Physical Sciences, Heriot-Watt University, Edinburgh, EH14 4AS, UK

Abstract

Flexible electronics is of considerable interest for many applications due to the distinctive features of low-cost, flexibility and light weight capabilities. However, in translating the technology from research to practical applications one faces many challenges. One of them is to formulate suitable ink materials where the selection of functional components, for example in the case of organic silver ink, the silver precursor, complexing agent and volatile organic solvent, are very critical because these constituents determine the final properties of the ink. In this paper, a new type of silver organic ink with decomposition and self-reduction mechanisms (10 wt% silver content) was formulated. It is shown that the ink is capable of producing silver films with good uniformity and conductivity on a polyimide substrate after sintering at 155 °C. The effect of solvent on the thermal property of the formulated ink have been investigated by differential scanning calorimetry (DSC) and UV-Vis spectrscopy, where the active roles of the solvents and the underlying chemical reactions in the ink during heating were studied. The reaction mechanism between the complexing agent and the silver precursor

*Corresponding author:

Dr Changhai Wang; Email:C.Wang@hw.ac.uk, Tel: +44 1314513903;

was confirmed by FT-IR measurements. The effects of sintering temperature and time on the microstructure and electrical properties of the silver ink films have been studied in detail using XRD, SEM/EDX and 4-probe based techniques. The defects such as voids and cracks as well as the coffee rings, which are often associated with films produced from organic silver inks, were reduced significantly by using both decomposition and self-reduction mechanisms in film formation.

Keywords: silver; conductive ink; electrical properties; microstructure; film

1. Introduction

With the development of industrial and consumer applications, electronic products based on glass and other conventional substrates can no longer meet the requirements of functionalities and convenience due to their weight and rigidity. Miniaturization and flexibility of electronic products are desirable but this tends to increase the cost of manufacture. As a potential solution, flexible electronic technology is capturing industry attention due to their features of low-cost, flexibility and lighter weight, which can manufacture products by printing functional conductive inks on a variety of flexible substrates. The technology enables many potential applications covering a wide range of electronic and energy storage devices as well as systems such as touch screens,[1] sensors,[2,3] transistors,[4] photovoltaic cells,[5] light-emitting diodes[6] and electrochemical energy storage systems.[7] Up to now, considerable effort has been devoted to the development of materials and processes for flexible electronics. However, much work is still necessary in order to realize wide applications, such as low cost and low temperature processing capabilities.

Conductive inks are important materials for flexible electronics since these can be used to produce conductor patterns with low cost methods such as inkjet printing. The ink

formulation is a key factor determining the development of flexible electronics, which should not only meet the demands of the large scale patterning process, but also provide the required electrical and mechanical performance. Currently, various kinds of conductive inks have been formulated by using polymers,[8] carbon nanotubes,[9,10] graphene[11] and metal nanoparticles or organic metal complexes[12-40] as fillers. Among these, silver based inks have been under rapid development due to their good electrical conductivity and strong anti-oxidant characteristics as compared with copper inks.[12, 13]

Silver organic inks, also known as particle free inks, have been developed because of the flexibility in preparation, stability and low cost as compared to the silver nanoparticle based ink. In general this type of ink is an organic silver salt based solution or silver-organic complex containing volatile organic solvents that provide essential rheological properties for patterning. Since the silver is usually in ionic forms in the ink, there is no aggregation issue during the preparation, storage and patterning process. After depositing onto substrates, the organic solvents evaporate leaving the silver salt as a deposit, which is subsequently decomposed in a thermal treatment process for formation of conductive metal patterns.

Favorable conductivity at low temperature (<150°C) is very desirable for flexible electronics as it would widen the applications of silver organic inks on polymer or paper substrates. Therefore, the selection of functional components such as silver precursors, complexing agents and volatile organic solvents is very critical because these determine the final thermal, electrical and mechanical properties of the ink. To date, silver nitrate,[20] silver acetate,[14,17] silver carbonate,[18] silver neodecanoate,[28] silver oxalate,[23] β-ketocarboxylate silver,[19] silver 2-[2-(2-methoxyethoxy)ethoxy] acetate,[32] silver

hexafluoroacetylacetonate cyclooctadiene[41] and silver citrate[27, 33] have been used as silver precursors to formulate organic silver inks. Each precursor has its advantages and disadvantages. For instance, the first three have a relatively high decomposition temperature and can decompose in the presence of light. β-ketocarboxylate silver and 2-[2-(2-methoxyethoxy)ethoxy] acetate silver are stable but the synthesis is relatively complex. Although Silver oxalate has lower decomposition temperature and highest silver content (71wt% silver), it is toxic, explosive and unstable in the presence of light. As for the volatile organic solvents, alcohols, especially low molecular weight ones, are usually preferred because they are less toxic and are easy to evaporate without leaving residues in the resulting film, which is beneficial for the final conductivity. Furthermore, they usually contain hydroxyl groups with a certain amount of reduction capability which is also beneficial for film formation. Among the complexing agents, amines, cyanides and thiocyanate are usually considered since they can solubilize and stabilize the silver precursors in the alcohols based solvents.

Compared with silver acetate, nitrate or carbonate, silver citrate seems to be an ideal precursor for use in silver organic ink, which were found to have excellent ink stability property as well as can promote silver reduction at lower temperatures.[27, 42] However, there are only two studies carried out using this material.[27, 33] Nie et al.[27] synthesized their ink using silver citrate as a precursor and 1, 2-diaminopropane as complex agent whereas Chen et al.[33] used silver citrate as a catalyst for the growth of copper films. Although interesting results have been obtained in both cases, there are still some areas to be studied. In the first case, the ink was formulated using only short chain alcohols as the solvents (methanol and isopropanol), which were not ideal. It is well known that films

derived from inks containing such solvents often suffer from serious coffee ring effects because these solvents can easily form an outward convective flow in the area contacting with a substrate during sintering; the flow causes the small particles formed in the ink droplet to move to the edge region, resulting in a ring shape pattern.[43] Also, there were no detailed description of ink formulation, film formation and conduction. Furthermore, the chemical reactions leading to ink formation based on such material (silver citrate) are not clear. In addition, the resultant film from such inks usually has voids and cracks due to bubbling effects[23] resulted from the fast solvent evaporation of these solvents and the decomposition of silver complex, which should be avoided. Last, the effects of the constituents such as solvents in the ink on its properties are rarely investigated. Therefore, it is necessary to develop a silver citrate based ink and elucidate its formulation and conductive mechanism as well as to investigate the role of each constituent in the ink.

In this paper, a silver organic ink with self-reducible and decomposable properties was formulated by a complexation process in mixed solvents using silver citrate as the silver precursor and ethylenediamine as the complexing agent. The resultant silver films have shown good conductivity after sintering at 155°C. The physical phase, chemical composition and thermal behavior of the silver citrate precursor have been studied in order to understand its function as an ink precursor. The effect of the solvent on the thermal property of the formulated ink was investigated to understand the chemical reactions in the film formation process. The effects of sintering temperature and time on the microstructure and electrical properties of the silver films from the ink have been investigated in detail. The voids and cracks, which are often present in the films due to

the bubbling effects, were effectively reduced by using the self-reduction mechanism in the film formation process.

2. Experimental Section

2.1 Materials

Silver nitrate ($AgNO_3$), sodium citrate tribasic dihydrate ($C_6H_5O_7Na_3 \cdot 2H_2O$), ethylenediamine ($C_2H_8N_2$), ethylene glycol ($C_2O_2H_6$) and 2-propanol ($C_3H_8O$) were obtained from Sigma-Aldrich and were used as received without further purification. The physical properties of the various solvents used in this study are listed in Table 1. The substrate was a Kapton polyimide film from DuPont (500 HN, 127 μm in thickness). Before application, the films of 15mm×15mm were cleaned with ethanol and de-ionized water to remove particles and organic contamination and dried in an oven.

Table 1. Physical properties of various solvents

Reagent	**Viscosity (η, mPa·s)**	**Surface tension (γ/mN·m^{-1})**	**Boiling point (T_b/°C)**	**ρ/g·cm^{-3}**	**Possible problem**
2-Propanol	2.431	21.7	82.45	0.7855	Coffee ring effect
Ethylene glycol	25.66	46.49	197.85	1.1115	Solvent contraction effect
Ethylene-diamine	1.7	42	116	0.90	/

2.2 Synthesis

The silver organic decomposition ink used in this study was prepared by dissolving the synthesized silver citrate into a mixture of organic solvents. The process is as follows: silver nitrate (1.7 g, 0.01 mol) and sodium citrate dehydrate (1.1 g, 0.0037 mol) were first dissolved in 30 ml of de-ionized water, respectively, then mixed by continuous stirring for 1 h at room temperature. The product, silver citrate, was collected by vacuum filtration

and then washed with de-ionized water for three times and ethanol for twice, dried at 40°C for 6 h in an oven and stored away from light. The obtained silver citrate powder was 1.603 g, which is less than the theoretical product (1.709g), this indicates that silver citrate is sparingly soluble in de-ionized water and ethanol.

For ink preparation, 0.5 g of the obtained silver citrate was dispersed in 2 ml of a mixed solvent containing 2-propanol (1.25 ml) and ethylene glycol (0.75 ml). After stirring for 10 minutes, ethylenediamine (0.5 ml) was added at once. The mixture was stirred for 60 minutes to form the ink, named as ink_1. It is useful to note that the appearance of the solution changed, from the initial suspension to a homogeneous transparent solution with an orange color. The silver content in the ink is about 10 wt%.

2.2 Ink deposition and sintering

The as-prepared ink was deposited on the PI films by a drop-coating method, and sintered at selected temperatures for up to 60 minutes. The film thickness was controlled by the volume of ink solution deposited onto the PI film.

2.3 Characterization

Ultraviolet-visible (UV-Vis) absorption spectra were recorded on a Lambda 25 UV-Vis spectrophotometer using water as solvent. Fourier transform infrared (FT-IR) spectra in the range of 400-4000 cm^{-1} were recorded on a Thermo Scientific Nicolet iS5 FT-IR spectrometer. The thermal profiles of the powder and ink were measured under nitrogen atmosphere by differential scanning calorimetry (DSC, TA instrument) using aluminum pans at a heating rate of 10 °C min^{-1} from room temperature to 250 °C and a nitrogen flow rate of 80 ml min^{-1}. X-ray diffraction (XRD) analysis was conducted by using Cu Kα and λ = 0.15418 nm. Grain sizes of silver crystallites were calculated using Scherrer's

formula. The morphologies of the silver films after sintering were observed on a FEI Quanta 3D Scanning Electron Microscope (SEM). The chemical composition was determined on an Oxford X-maxN 150 surface energy disperse spectrometer (EDX). The sheet electrical resistivity was measured using a 4-point probe method (Jandel Engineering, UK). The thickness of the sintered films was measured using a Zygo View 5200 white light phase shifting interferometer and was used to calculate the equivalent bulk resistivity.

3. Results and discussion

3.1 Characterization of silver precursor

Silver citrate was chosen as the silver precursor since it has a relatively lower decomposition temperature, which is beneficial in ink application to substrates such as some temperature-sensitive polymer or paper substrates. Also, this compound contains one OH group that can increase its solubility in alcohols. The silver citrate used in this study was prepared through a typical ion exchange method as shown below:

$$Na_3C_6H_5O_7 + 3AgNO_3 \rightarrow Ag_3C_6H_5O_7 + 3NaNO_3$$

As an important component of the ink, the characteristic of the as-prepared silver citrate powder was investigated by FT-IR, XRD, EDX and DSC-TG to confirm its physical phase, chemical composition, and thermal decomposition temperature.

Fig. 1 shows the XRD pattern of the as-prepared silver citrate powder measured in 2θ from 20° to 85°. The main peaks appeared at 7.749°, 15.003°, 21.603°, 29.062°, 31.249°, 38.783°, 43.951° and 48.375°. The data are in good agreement with the JCPDS No.01-0030 for silver citrate. No diffraction peaks from any other impurities were

detected, indicating that the above reaction took place completely and the silver citrate powder was prepared successfully.

Fig. 2a shows the IR spectrum of the as-prepared silver citrate powder. A broad feature around 3200 cm^{-1} is attributed to the O-H stretching vibration. Two sharp bands at 1537 and 1401 cm^{-1} are attributed to the asymmetric stretch vibration and the symmetric stretch vibration of C=O in the carboxyl group (-COO-), respectively. The band at 1073 cm^{-1} is from C-O stretch. These features confirm that silver citrate has a structure of carboxylates.

It has been reported that the wave number difference (Δ) between the asymmetric ν_{as} CO_2^- stretch peak and the symmetric ν_s CO_2^- stretch peak in the carboxylate complex can be used to identify the type of interaction between the carboxylate moiety and Ag^+ ions.[44] Unidentate complexes exhibit the largest Δ values (200-320cm^{-1}). Chelating (bidentate) complexes have the smallest Δ values (<110cm^{-1}). The medium Δ values (140-190 cm^{-1}) for bridging complexes are greater than those of chelating complexes, and close to the ionic values. Based on these observations, we conclude that the carboxylate moiety and Ag^+ ions interacts in a bridge manner (Δ value: 1537-1401 = 136cm^{-1}).

The chemical composition was identified by EDX as shown in Fig. 2b. Evidently, three elements (C, O, and Ag) exist in the powder as expected from the chemical structure.

Fig. 3 shows the thermal behavior of the as-prepared silver citrate powder. The DSC curve shows an endothermic peak at 198°C, relating to the thermal decomposition of the silver citrate, which is similar to the behavior of other silver carboxylates but the decomposition temperature is lower than that of them.[23] This is a preferred property. From the TG curve, it can be seen that the powder starts to lose weight at 175°C and a maximal

rate of weight loss occurs at 200°C. The total weight loss was about 40 wt%, indicating that the left weight is 60wt%. This is basically in line with the proportion occupied by silver in the silver citrate (63.19wt%). All of the results demonstrate that silver citrate is an ideal ink precursor material.

3.2 Ink formulation

For ink preparation, ethylenediamine, a small molecule bi-dentate aliphatic amine with low boiling point (116°C), was chosen as the ligand to increase the silver content of the ink since it can form a complex that has higher solubility than pure silver citrate) and to improve film formation efficiency as well as to decrease the ink sintering temperature.[45] Less organic content in the metal-ligand complex can make the sintering process easier and faster since the energy and time required to evaporate the organic content are reduced.[42] 2-Propanol, a volatile alcohol, was used as the ink solvent to adjust the rheological properties as it has lower surface tension and viscosity, which is beneficial to ink deposition. Ethylene glycol was selected as a reduction agent and a co-solvent with a high boiling point to suppress the undesirable coffee ring effect caused by 2-propanol in film sintering process.[17] The preparation details were given in the experimental section and the prepared ink was named as ink_1.

The sparingly soluble silver citrate can be dissolved in the organic solution containing ethylenediamine with no difficulty, mainly via the following complexing process, resulting in a soluble complex.

$$Ag_3C_6H_5O_7 + 3C_2H_8N_2 \rightarrow Silver\text{-amine } complex$$

FT-IR was employed to investigate and confirm this complexation mechanism. As the solvents will have some influence in both spectra, the complex was prepared using

only silver citrate and ethylenediamine in a stoichiometric ratio without adding any solvents. It was found that the solid silver citrate became dissolvable when ethylenediamine was added, indicating that the above reaction occurred. The silver amine complex formed from ethylenediamine will go through the later sintering process.

Fig. 4a shows the IR spectrum of ethylenediamine. The absorption peaks at 3352 and 3276 cm^{-1} correspond to the asymmetric and symmetric stretch of the NH_2 groups. The two peaks at 2920 and 2852 cm^{-1} are assigned to the asymmetric CH_2 stretch and the symmetric CH_2 stretch. The peak at 1594 cm^{-1} is associated with NH_2 bending vibration. Fig. 4b shows the spectrum of the complex. It is worth noting that a new OH stretching vibration peak and a new C-O stretching vibration peak appear at 3675 cm^{-1} and 1059 cm^{-1}, respectively, which are from the silver citrate. In combination with the FT-IR spectrum of silver citrate powder, it can be seen that the positions of these two peaks change, which might be the result of complexation between silver atom and amino group. All peaks associated with NH_2 group have a red-shift, from 3352 to 3339 cm^{-1}, 3276 to 3269 cm^{-1} and 1594 to 1556 cm^{-1}, implying that a coordination process occurred on the bond of NH_2. Herein, ethylenediamine can donate electron from the amino group to the silver atom of silver citrate, decreasing the electron density of the amino group and thus resulting in red-shift of the NH_2 stretch. These changes indicate that the ethylenediamine forms a complex with silver citrate.

3.3 Effects of solvent on the thermal behavior of the ink

The solvent used in the ink determines the quality of the resultant films and should meet various requirements, such as stability, uniform surface morphology of the formed film and conductivity.

Ethylene glycol is a reduction agent that can reduce silver ions by generating glycolaldehyde at a relatively lower temperature (150°C).[18] In order to investigate whether this mechanism is still active in ink_1 and to better understand the effect of the solvent on thermal decomposition, an ink, named Ink_0 was prepared using the same ink formulation method but replacing ethylene glycol with ethanol. DSC analysis was carried out to investigate the thermal decomposition behavior of both inks and the results are shown in Fig. 5.

The DSC curves of Ink_0 show two major endothermic peaks at 62°C and 155°C. The first one is attributed to solvent evaporation. Since the ink color changes from initially orange to black, and then to metallic silver during the heating process (Fig.5a), it can be deduced that the second peak arises from the decomposition of the complex. Based on the results of the previous studies reported in [46] and the color of silver oxide, the color change should be associated with the transition of silver ion complex to silver oxide and finally to elemental silver.

$$Silver\text{-}a\min e\ complex \xrightarrow[decompositon]{Thermal} Ag_2O \rightarrow Ag(s)$$

However, the ink containing ethylene glycol (Ink_1) shows different behavior, although the ink color changes were similar to that of ink_0 in the sintering process. The first peak below 50°C is attributed to the evaporation of 2-propanol. The second and third peaks, appeared at 130°C and 145°C, are new peaks. From the work in [18], below 150°C ethylene glycol can decompose to glycolaldehyde that can reduce silver ions to metallic silver. So these two peaks are attributed to the decomposition of ethylene glycol and reduction of the complex ion or Ag_2O derived from the above reaction. Therefore, it can be deduced that the reduction effect of ethylene glycol works in this system.

$$HOCH_2CH_2OH \xrightarrow{Heating>130^{\circ}C} CH_3CHO + H_2O$$

$$Silver\text{-}a\min e\ complex + CH_3CHO \xrightarrow{Reduction} 3Ag(s)$$

$$Ag_2O + CH_3CHO \xrightarrow{Reduction} Ag(s)$$

From the above analysis, it can be concluded that two reaction processes are simultaneously active in our ink system: (1) decomposition and (2) reduction. The latter is the dominant effect. Therefore the ethylene glycol not only acts as the co-solvent but also functions as a reduction agent. This is different from previous work which was based only on the decomposition effect.[27] The decomposition and reduction temperature are both lower than that of the silver citrate powder.

UV-Vis absorption peaks are sensitive to the metal nanoparticles, and this is especially true for silver nanoparticles. The UV-Vis technique can be used to detect the atomic, ionic, and cluster states of silver, which exhibit different characteristic absorption bands.[46] The absorption band of Ag^+ ions is in the 190-230 nm spectral range, silver atoms Ag^0 (or containing Ag_2O) absorb in the 250-330 nm region, and small Ag_n clusters at 330-360 nm and 440-540 nm. Light absorption by silver nanoparticles manifests pronounced resonance bands at 380-450 nm due to the excitation of surface plasmon resonances (SPRs).[47] Therefore, UV-Vis spectroscopy was employed to study the temperature dependent absorption characteristics as shown in Fig. 6.

From results in Fig. 6, it can be seen that at temperatures below 125°C, there is only one sharp absorption band around 240 nm, which is from the complex according to previous description.[46] However, when the ink is heated above 145°C, the absorption band at 240 nm broadens and two new absorption bands appear at 330 nm and 386 nm. These

bands are associated with the formation of Ag_2O, silver atoms or silver clusters and silver nanostructures, respectively. In other words, the complex is reduced and decomposed into elemental Ag.

Based on these results, it can be deduced that our ink underwent simultaneous the change of solvent components and the decomposition/reduction of silver complex at elevated temperatures. In the process ethylene glycol generates glycolaldehyde and triggers the reduction of the silver ion complex or Ag_2O to Ag.

3.4 Effects of sintering temperature on microstructure and chemical composition of silver films

Silver films were produced by drop-coating of ink_1 on the cleaned PI substrates. The sintering process was carried out on a hotplate in a chamber. Based on the DSC results and UV-Vis analysis of the ink, selected temperatures between 125 °C and 200 °C were used for the thermal sintering. XRD, SEM/EDX and Zygo interferometer were used to evaluate the produced silver films.

Fig. 7 shows the optical image of ink_1 and a corresponding silver film surface profile (sintered at 230 °C) where the thickness was about 2.5±0.5μm. The optical image of silver films produced from Ink_0 was also given for comparison. Clearly, the film from Ink_1 has a continuous surface without pores or a coffee ring effect of ink_0 resulted by fast evaporation of solvents with lower boiling point, indicating the positive effect of ethylene glycol as a co-solvent.

Fig.8 shows the crystalline structure of the silver films obtained at different sintering temperatures for 60 min. Diffraction peaks were observed at 2θ values of 38.2°, 44.4°, 64.5°, 77.5° and 81.6° and were the same in all of the films. The results indicate that the

complex was transformed to silver crystals. The diffraction peaks are indexed as the (111), (200), (220), (311) and (222) crystal planes of the face-centered cubic (fcc) crystal structure.

The crystallite sizes of the silver nanoparticles in the films formed at 125 °C, 155 °C and 185 °C were calculated using the Debye-Scherrer equation,[39]

$$d = 0.89\lambda / \beta \cos\theta \qquad (1)$$

where d is the particle size, λ is the x-ray wavelength (0.15418 nm), θ is the Bragg angle and β corresponds to the full width at half-maximum (FWHM). The results are given in Table 2.

Table 2. Particle sizes of silver nanocrystals in the film at different sintering temperatures

Sintering temperature (°C)	2θ (Degrees)	FWHM (Å)	Size (nm)
125	38.274	0.314	26.11
155	38.403	0.289	28.98
185	38.238	0.278	29.34

The average particle size of silver nanocrystals in the film increases with the sintering temperature.

Fig. 9 shows the SEM images of the silver films sintered at different temperatures. It can be seen that the morphology of the films changes with the sintering temperature, which is a result of the fast evaporation of solvent and thermal decomposition and reduction of the complex. At lower sintering temperatures (125°C, 140°C), the films show voids and cracks (Fig. 9 a and a_1) and silver nanoparticles produced are small. As the film is partly wet at 125°C, these nanoparticles were still to be surrounded by organic molecules as will be shown in the results of EDX measurements. At the sintering

temperatures of 155°C and 170°C, the defects on the film surface become less pronounced and the grain boundary becomes obvious (Fig.9d). Sintering at higher temperatures (180°C, 200 °C) leads to larger silver nanoparticles formed through neck connection (Fig. 9 e_1 and f).

In the previous work by Dong et al.,[23] fast solvent evaporation and bubbling caused by CO_2 or H_2O formation from decomposition of the silver complex were the reason for pores and cracks in the silver films. However this phenomenon is not obvious in our ink system. It is believed that this is suppressed by a simultaneous self-reduction mechanism during film formation and the decomposition effect. The self-reduction effect due to the presence of ethylene glycol produces silver nanoparticles that fill in the pores and cracks, compensating for the bubbling from the decomposition of the silver salt. This is a key advantage of the new ink developed in this work.

The sintering temperature plays two roles in the film formation process: (1) it aids solvent evaporation and (2) it triggers chemical reactions in the ink to produce silver nanoparticles and subsequently nanocrystals.

Fig. 10 shows the C and Ag content in the sintered films as obtained from the EDX data. As shown in Fig. 10 the C content decreases rapidly as the sintering temperature was increased from 125°C to 200°C, indicating that the decomposition and volatilization of organic molecules mainly occurred at this stage. The Ag content increased from 72.63 wt% to 88.5 wt% over the same temperature range. This indicates that most of the organic molecules were decomposed and vaporized and the Ag^+ ions were reduced to Ag.

3.5 Effects of sintering time on microstructure and chemical composition of silver ink films

The effect of sintering time on the microstructure of silver films from ink_1 was also investigated. The samples were obtained by heating the ink_1 films on PI substrates at 155°C for 5, 15, 30 and 60 minutes and were then evaluated by SEM, XRD and EDX methods.

As shown in Fig. 11, silver ions could be transformed to silver nanocrystals within 5 minutes. With increasing sintering time, the intensity also increases, indicating that more metallic silver was formed. The particle sizes of silver nanocrystals in the films were calculated using equation (1) and the results are shown in Table 3. The increase in particle size as the heating time increases is very small. This means that the nucleation and growth of silver nanocrystals is less dependent on the heating time.

Table 3 Particle size of silver nanocrystals in the films processed at 155°C for different times

Sintering time (min)	2θ (Degrees)	FWHM (β)	Size (nm)
10	38.210	0.294	27.63
45	38.164	0.286	28.24
60	38.403	0.289	28.98

The SEM images in Fig. 12 show the microstructures of the silver films produced at 155°C for different times. Some differences in the morphologies can be observed. The film heated for 5 min has some cracks on its surface. Silver nanoparticles produced seem to be surrounded or covered by organic molecules (Fig. 12a). With increasing time, the films show relatively more compact microstructures consisting of small silver particles with better film uniformity (Fig. 12b). The film sintered for 30 min has a porous surface profile consisting of many silver particles. The grain boundaries become less obvious. More particles are in contact at this time (Fig. 12 c and c_1). When the sintering time

reaches 60 minutes, more silver nanoparticles are produced to form larger silver nanoparticles and produce a relatively complete film (Fig. 12 d and d_1).

As discussed before, the film morphology is dependent on the solvent evaporation rate and thermal decomposition or reduction of the silver-amine complex. At 155°C, the solvent evaporates quickly resulting in an uneven film when the sintering time was 5 minutes. As will be shown in section 3.6, the film conductivity was low indicating insufficient formation of Ag particles from the complex. For the sintering time of 15 minutes, the film is less uneven as there is material redistribution due to decomposition and reduction of the complex in the film. Further increase in sintering time results in improved surface morphology (Fig. 12 c and d).

EDX analysis was also used to illustrate this phenomenon, as shown in Fig. 13. Clearly, three elements (C, O, and Ag) were found in the films after heating at 155°C. As the heating time was increased from 5 to 60 minutes, the Ag content increased from 81.70 wt% to 86.28 wt% and the content of C decreased from 12.37 wt% to 8.86 wt% while the oxygen content decreased from 5.93 wt% to 4.86 wt%. The results indicate that the organic molecules were decomposed and volatilized mostly within 15 minutes and the decomposition or reduction reaction of the complex continued to a large extent within 60 minutes.

3.6 Electrical performance

The resistivities of the silver films obtained by heating at various temperatures for 60 minutes were calculated from the measured sheet resistance and film thickness using the following equation,

$$\rho = R_s \cdot t \qquad (2)$$

where ρ is the resistivity, R_s is the sheet resistance of the Ag film, t is the average thickness of the film which was measured to be about 2.5±0.5 μm.

The calculated resistivity values are shown in Fig.14 as a function of sintering temperature. It can be seen that the resistivity decreases rapidly by several orders of magnitude from 0.4 Ω·cm at 125 °C to 3.9×10^{-5} Ω·cm at 200°C. Below 125 °C, the film was not totally dry and showed a high resistivity that is beyond the sensitivity of the 4-probe instrument. The resistivity decrease can be explained based on the effects of the temperature in the film formation process. At lower temperature, not all solvent has evaporated and the formation of silver is not complete, so the film has high resistivity. Conversely, at higher temperature, solvent evaporation is fast and more silver nanocrystals can be formed to improve the stacking density of Ag nanoparticles in the film. The pores are eliminated by using both decomposition and self-reduction effects in the sintering process. A continuous and uniform film with better particle stacking density is obtained and hence good film conductivity. It is worth noting that film resistivity of 10^{-5} Ω·cm can already be achieved at sintering temperatures below 150°C. This shows that the organic silver ink can be compatible with the temperature sensitive flexible substrates such as PET or PEN.

The resistivities of the films heated at 155°C for different times are shown in Fig. 15. The resistivity decreases by only one order of magnitude from 1.34×10^{-4} Ω·cm to 7.94×10^{-5} Ω·cm when the sintering time increases from 5 to 60 minutes. This is in agreement with previous analysis of film formation based on the decomposition or reduction of the complex as described in section 3.5.

3.7 Mechanism of silver film formation

Based on the above analysis, it is clear that the electrical performance is correlated with the microstructural features of each film. So it is necessary to understand the underlying mechanism. The sintering of the decomposable organic silver ink is generally considered as a particle formation process after solvent evaporation.[48] When the ink deposit is heated, the decomposition of the silver precursor generally starts at the temperature above the boiling point and the decomposition temperature of the solvent. Therefore, in most cases, silver particles are produced in situ in the absence of solvent. However, as the ink formulation and the parameters used in the sintering process are usually different, the evolution of the microstructures is also different.

According to the DSC results and the physical properties of the chemicals used (Table 1), the process of film formation can be illustrated using the schematic diagram shown in Fig.16.

When the sintering temperature is around 125°C, evaporation of solvent is dominant with 2-propanol and the unreacted ethylenediamine evaporating rapidly due to their low boiling points (82.45 °C and 116 °C, respectively) . Usually, this evaporation can induce a vapor recoiling force at the interface with the substrate, pushing the liquid droplets into isolated islands, and finally forming clusters of various sizes (Fig. 16b). Due to the high thermal stability of the silver complex, the solvent would evaporate in each cluster before decomposing. If there is no high boiling point solvent in the ink, the silver particles produced by thermal decomposition of the silver complex would be largely restricted in these isolated islands and a discontinuous film is formed. Ideally, a sufficient amount of unevaporated solvent should be left in the film when the thermal decomposition of silver complex begins. In our ink system, as ethylene glycol has a relatively high boiling point

(T_b=197.85 °C) and therefore it is left in the film to facilitate decomposition of the silver organic complex to silver nanoparticles, resulting in a continuous microstructure. However, due to the low heating temperature, fewer silver NPs are produced, which are still coated by organic molecules; a conductive film cannot be formed. Therefore, the electrical performance was poor and the sheet resistance was too high to be measured by the 4-probe device.

When the temperature is increased to 155°C, the silver complex starts to decompose into Ag_2O. At the same time the glycolaldehyde as produced by ethylene glycol, reduces the Ag_2O and the silver complex into silver nanoparticles (Fig. 16c) serving as nucleus for the subsequent thermal decomposition event. In addition, the thickness of the surrounding organic layer separating the silver particles is also decreased due to the evaporation and decomposition effects, which enables the quantum tunneling effect to occur.[49] Meanwhile, the pores and voids among the NPs become decrease in quantity and size so a homogeneous film with densely packed silver nanoparticles is formed (Fig. 16d). Hence good film conduction (low resistivity) is obtained.

At sintering temperatures above 155°C, further improvement in film quality and conductivity can be obtained but the resistance of the film decreases slowly, indicating that almost no solvent is left in the film and all Ag^+ ions have been reduced to Ag^0.

4. Conclusions

In summary, using ethylenediamine as a complexing agent, an organic silver ink with self-reducible and decomposable mechanisms for film formation has been achieved. The results show that good film conductivity can be obtained at a low sintering temperature of 155°C, with a resistivity value of 7.94×10^{-5} Ω·cm. Defects such as pores and cracks as

well as the coffee ring effect which are often associated with films from organic silver inks, have been reduced or eliminated by using mixed solvents containing active components. This is achieved by exploiting both self-reduction and decomposition mechanisms in the film formation process. The active role of ethylene glycol in the ink solvents and the underlying chemical changes during the heating process were clarified, where the ink underwent simultaneous the change of solvent components and the decomposition/reduction of silver complex at elevated temperatures. The effects of sintering temperature and time on the microstructure and electrical properties of the silver ink films have been studied in detail and the relationship between them was demonstrated. The residual level of organic solvents, the decomposition/reduction degree of silver-amine complex as well as contact area of produced silver nanoparticles, are three dominating influence factors on the conductivity of silver films.

Acknowledgement

The authors are grateful to Mr Mark Leonard and Dr Jim Buckman for their assistance in the surface profilometry and EDX work respectively. Wendong Yang was supported by an EPSRC DTP studentship.

References

[1] J. Lee, P. Lee, H. B. Lee, S. Hong, I. Lee, J. Yeo, S. S. Lee, T. S. Kim, D. Lee, S. H. Ko, Adv. Funct. Mater 23, 4171 (2013)

[2] X. Liao, Q. Liao, X. Yan, Q. Liang, H. Si, M. Li, H. Wu, S. Cao, Y. Zhang, Adv. Funct. Mater 25, 2395 (2015)

[3] N. Dossi, F. Terzi, E. Piccin, R. Toniolo, G. Bontempelli, Electroanalysis 28, 250 (2016)

[4] Y. Jung, C. Yeom, H. Park, D. Jung, H. Koo, J. Noh, D. Wang, G. Cho, Organic Electronics 28, 197 (2016)

[5] T. M. Eggenhuisen, Y. Galagan, A. F. K. V. Biezemans, T. M. W. L. Slaats, W. P. Voorthuijzen, S. Kommeren, S. Shanmugam, S. Teunissen, A. Hadipour, W. J. H. Verhees, S. C. Veenstra, M. J. J. Coenen, J. Gilot, R. Andriessen, W. A. Groen, J. Mater. Chem. A 14, 7255 (2015)

[6] J. Liang, L. Li, K. Tong, Z. Ren, W. Hu, X. Niu, Y. Chen, Q. Pei, ACS Nano 8, 1590 (2014)

[7] H. Gwon, H. S. Kim, K. U. Lee, D. H. Seo, Y. C. Park, Y. S. Lee, B.T. Ahn, K. Kang, Energy Environ. Sci 4, 1277 (2011)

[8] N. Perinka, C. H. Kim, M. Kaplanova and Y. Bonnassieux, Physics Procedia 44, 120 (2013)

[9] W. R. Small, M. in het Panhuis, Small 3, 1500 (2007)

[10] J. W. Han, B. Kim, J. Li, M. Meyyappan, Mater Res Bull 50, 249 (2014)

[11] J. T. Li, F. Ye, S. Vaziri, M. Muhammed, M. C. Lemme, M. Ostling, Adv Mater 25, 3985 (2013)

[12] R. V. K. Rao, V. K. Abhinav, P. S. Karthik, S. P. Singh, RSC Advances 5, 77760 (2015)

[13] A. Kamyshny, S. Magdassi, Small 10, 3515 (2014)

[14] S. B. Walker, J. A. Lewis, J. Am. Chem. Soc 134, 1419 (2012)

[15] R. Shankar, L. Groven, A. Amert, K. W. Whites, J. J. Kellar. J. Mater. Chem 21, 10871 (2011)

[16] B. Y. Ahn, D. J. Lorang, J. A. Lewis, Nanoscale 3, 2700 (2011)

[17] W. D. Yang, C. Y. Liu, Z. Y. Zhang, Y. Liu, S. D. Nie. J. Mater. Chem 22, 23012 (2012)

[18] Y. Chang, D. Y. Wang, Y. L. Tai, Z. G. Yang. J. Mater. Chem 22, 25296 (2012)

[19] C. N. Chen, T. Y. Dong, T. C. Chang, M. C. Chen, H. L. Tsai, W. S. Hwang, J. Mater. Chem 33, 5161 (2013)

[20] Q. J. Huang, W. F. Shen, W. J. Song, Chem. Mater 22, 3067 (2010)

[21] W. D. Yang, C. Y. Liu, Z. Y. Zhang, Y. Liu, S. D. Nie, RSC Advances 4, 60144 (2014)

[22] S. Jeong, S. H. Lee, Y. Jo, S. S. Lee, Y. H. Seo, B. W. Ahn , G. Kim, G. E. Jang, J. U. Park, B. H. Ryu, Y. Choi, J. Mater. Chem. C 1, 2704 (2013)

[23] Y. Dong, X. D. Li, S.H. Liu, Q, Zhu, J.G. Li, X. D. Sun, Thin Solid Films 589, 381 (2015)

[24] Q. J. Huang, W. F. Shen, Q. S. Xu, R. Q. Tan, W.J. Song, Mater Chem Phys 147, 550 (2014).

[25] J. T. Wu, S. L. C. Hsu, M. H. Tsai, Y.F. Liu, W. S. Hwang, J. Mater. Chem 22, 15599 (2012).

[26] D. Y. Wang, Y. Chang, Q. S. Lu, Z. G. Yang, Mater Tech: Adv Perform Mater 30, 54 (2015)

[27] X. L. Nie, H. Wang H, J. Zou. Appl. Sur. Sci 261, 554 (2012)

[28] A. L. Dearden, P. J. Smith, D.-Y. Shin, N. Reis, B. Derby, P. O'Brien, Macromol. Rapid Commun 26, 315 (2005)

[29] Y. H. Choi, J. Lee, S. J. Kim, D. H, Yeon, Y. Byun, J. Mater. Chem 22, 3624 (2012).

[30] Y. I. lee, Y. H. Choa, J. Mater. Chem 22, 12517 (2012)

[31] T. Yonezawa, H. Tsukamoto, Y. Q. Yong, M. T. Nguyen, M. Matsubara, J. Mater. Chem6, 12048 (2016).

[32] S. F. Jahn, T. Blaudeck, R. R. Baumann, A. Jakob, P. Ecorchard, T. Ruffer, H. Lang, P. Schmidt, Chem. Mater. 22, 3067 (2010)

[33] J. J. Chen, J. Zhang, Y. Wang, Y. L. Guo, Z. S. Feng. J. Mater. Chem. C 4, 10494 (2016)

[34] D. Y. Deng, Y. R. Cheng, Y. X. Jin, T. K. Qi, F. Xiao. ACS Appl. Mater. Interfaces 5, 3839 (2013)

[35] Y. Hokita, M. Kanzaki, T. Sugiyama, R. Arakawa, H. Kawasaki, ACS Appl Mater Interfaces7, 19382 (2015)

[36] D. H. Shin, S. Woo, H. Yem, M. Cha, S. Cho, M. Kang, S. Jeong, Y. Kim, K. Kang, Y. Piao, ACS Appl Mater Interfaces 6, 3312 (2014)

[37] B. Y. Wang, T. H. Yoo, Y. W. Song, D. S. Lim, Y. J. Oh, ACS Appl. Mater. Interfaces, 5, 4113 (2013)

[38] Y. Farraj, M. Grouchko, S. Magdassi, Chem. Commun 51, 1587 (2015)

[39] Y. Tao, B. Wang, L. Wang, Y. Tai, Nanoscale Res Lett 8, 1 (2013)

[40] A. Yabuki, Y. Tachibana, I. W. Fathona, Mater Chem Phys 148, 299 (2014)

[41] K. Black, S. Jetinder, M. Danielle, S. Sarah, J. C. Sutcliffe, R. P. Paul, Scientific reports 6, 1 (2016)

[42] K. Zope, Novel synthesis of a solid silver oxalate complex used for printing conductive traces. (Thesis of Rochester Institue of Technology, 2017).

http://scholarworks.rit.edu/theses/9381. Accessed 11 Januraury 2017

[43] J. D. Torrey, T. L. Kirschling, L. F. Greenlee, J Res Natl Inst Stand Technol 120, 1 (2015)

[44] N. Wu, L. Fu, M. Su, M. Aslam, K.C. Wong, V. P. Dravid, Nano Lett. 4, 383 (2004)

[45] Y. Tao, B. Wang, L. Wang, Y. Tai, Nanoscale Res Lett 8, 1 (2013)

[46] G. Corro, U. Pal, E. Ayala, E. Vidal, Catal. Today 212, 63 (2013)

[47] M. Nadafan, R. Malekfar, A. Izadi-Darbandi, Z. Dehghani, Desalination Water Treat 57, 21286 (2016).

[48] Y. Dong, X. Li, S. Liu, Q. Zhu, M. Zhang, J. G. Li, X. Sun, Thin Solid Films 616, 635 (2016)

[49] X. W. Hu, L. H. Li, S. M. Zhao, X. Leng. Adv Mater Res 577, 287 (2011)

Figures Captions

Fig.1. XRD pattern of the as-prepared silver citrate powder

Fig.2. FT-IR spectrum and EDX results of the synthesized silver citrate powder.

Fig.3. DSC-TG curve of silver citrate powder

Fig.4. FT-IR spectra of the ethylenediamine and Silver-amine complex

Fig.5. (a) Optical images of ink_0 color change during the heating process, (b) DSC curves of the ink with and without ethylene glycol

Fig.6. UV-Vis absorption spectra of silver citrate ink obtained at different temperatures

Fig.7. (a) As-prepared ink_1; (b) Surface profile of a sintered silver film from ink_1; (c) Optical images of silver films produced from ink_0 and ink_1; (d) SEM images of silver

films produced from ink_0

Fig.8. XRD patterns of the silver films obtained at different sintering temperatures for 60 minutes. Data shifted vertically, for clarity.

Fig.9. SEM images of silver films sintered for 60 minutes, (a) 125°C, (b) 140°C, (c) 155°C, (d) 170°C, (e) 185°C and (f) 200°C (a_1 and e_1 are high magnification images of a and e).

Fig.10. C and Ag content from EDX results in the films as a function of sintering temperature

Fig.11. XRD patterns of Ag films prepared at 155°C for 5, 15, 30 and 60 min respectively

Fig.12. SEM images of silver films produced at 155 °C for 5, 15, 30 and 60 minutes (a-d, c_1 and d_1 are high magnification image of c and d)

Fig.13. EDX results of silver films produced at 155°C for 5, 15, 30 and 60 minutes (a-d)

Fig.14. Resistivity of the silver films sintered at various temperatures for 60 minutes

Fig.15. Resistivity of the Ag films as a function of heating time at 155°C

Fig.16. Schematic illustration for the film formation process of the silver ink

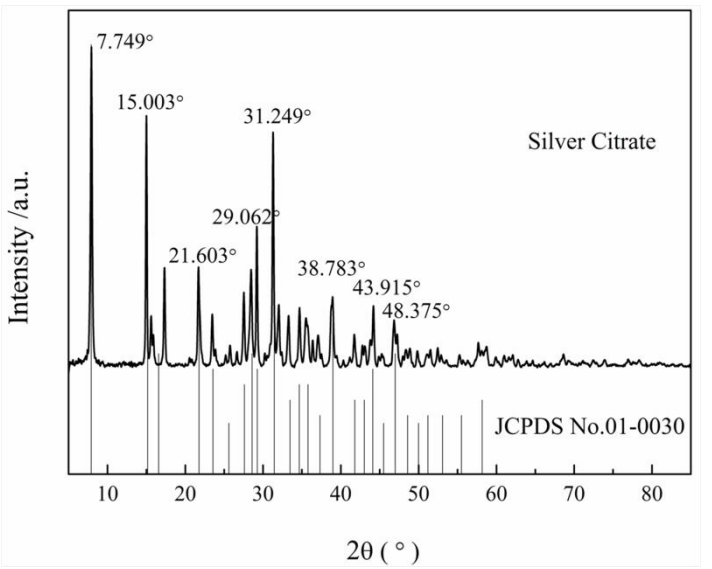

Fig.1. XRD pattern of the as-prepared silver citrate powder

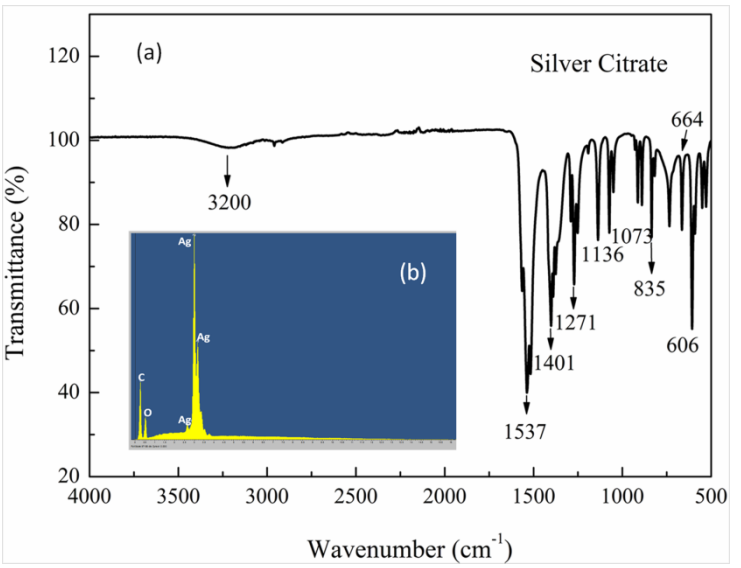

Fig.2. FT-IR spectrum and EDX results of the synthesized silver citrate powder.

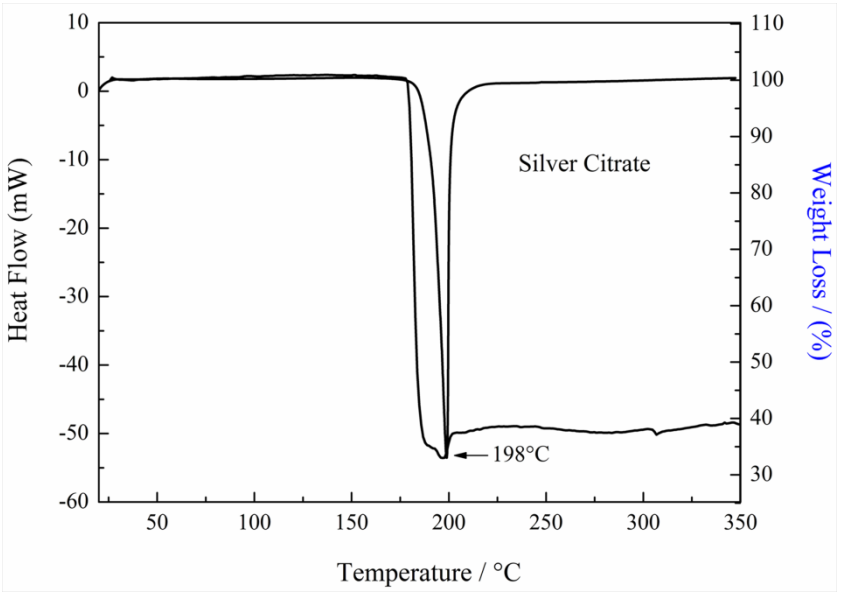

Fig.3. DSC-TG curve of silver citrate powder

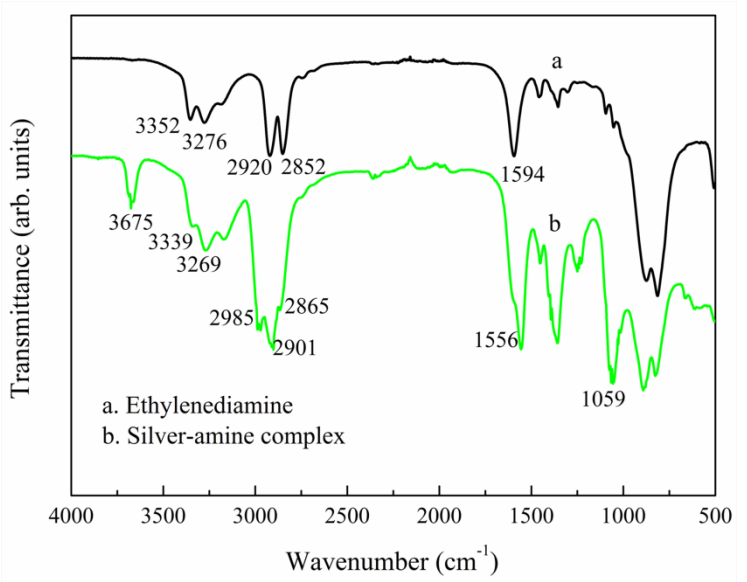

Fig.4. FT-IR spectra of the ethylenediamine and silver-amine complex

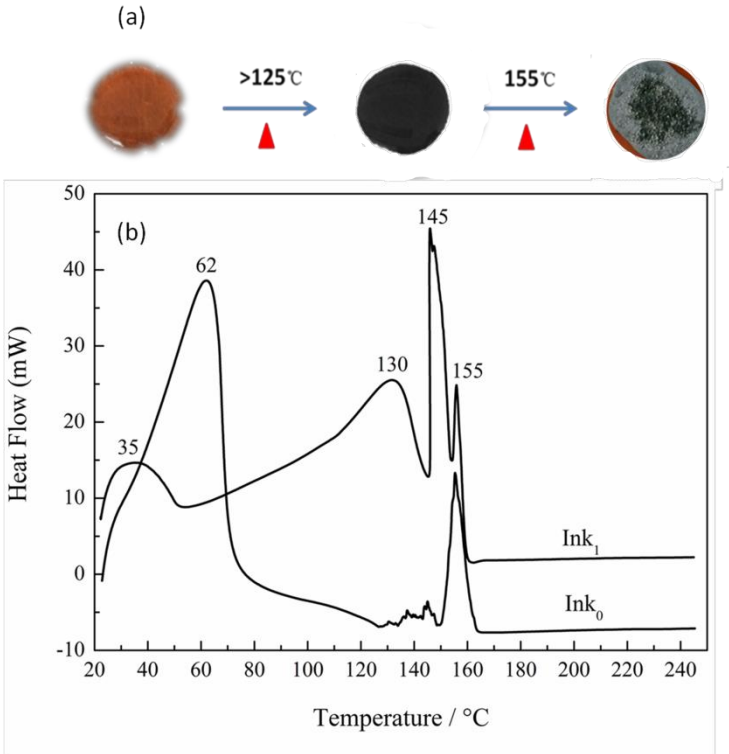

Fig.5. (a) Optical images of ink_0 color change during the heating process, (b) DSC curves of the ink with and without ethylene glycol

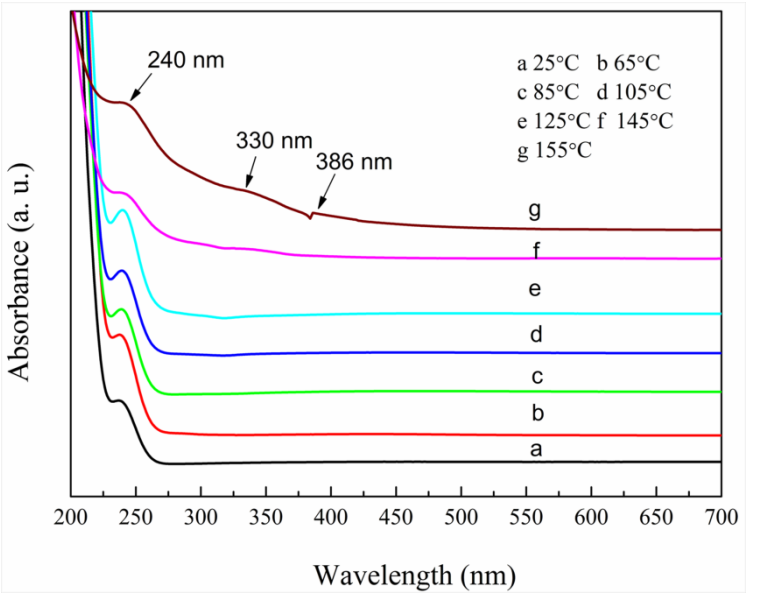

Fig.6. UV-Vis absorption spectra of silver citrate ink obtained at different temperatures

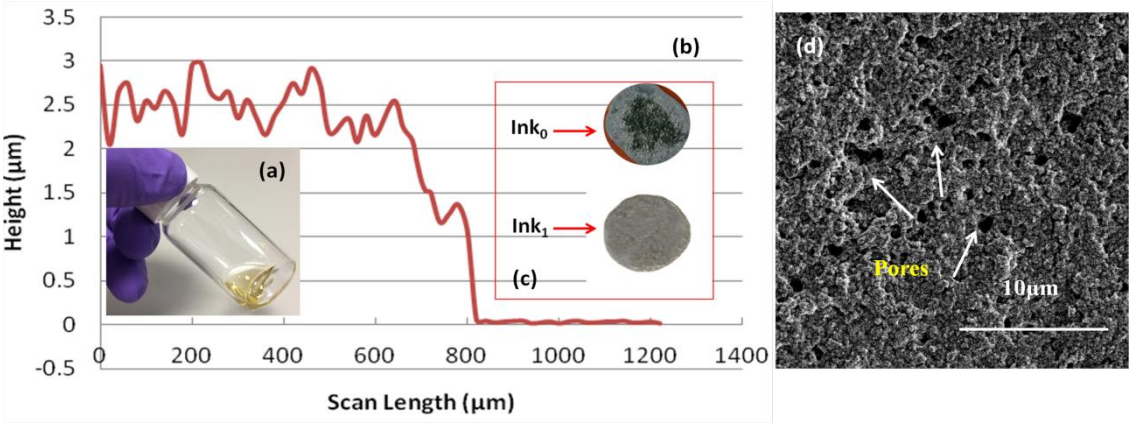

Fig.7. (a) As-prepared ink_1; (b) Surface profile of a sintered silver film from ink_1; (c) Optical images of silver films produced from ink_0 and ink_1; (d) SEM images of silver films produced from ink_0

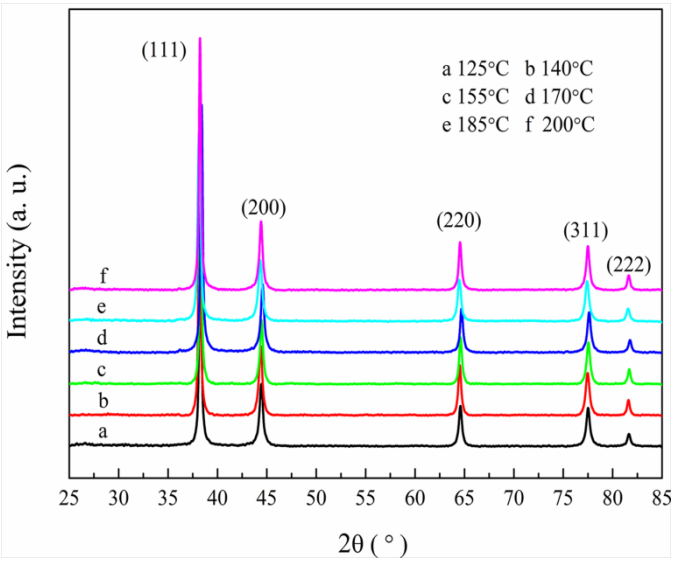

Fig.8. XRD patterns of the silver films obtained at different sintering temperatures for 60 minutes. Data shifted vertically, for clarity.

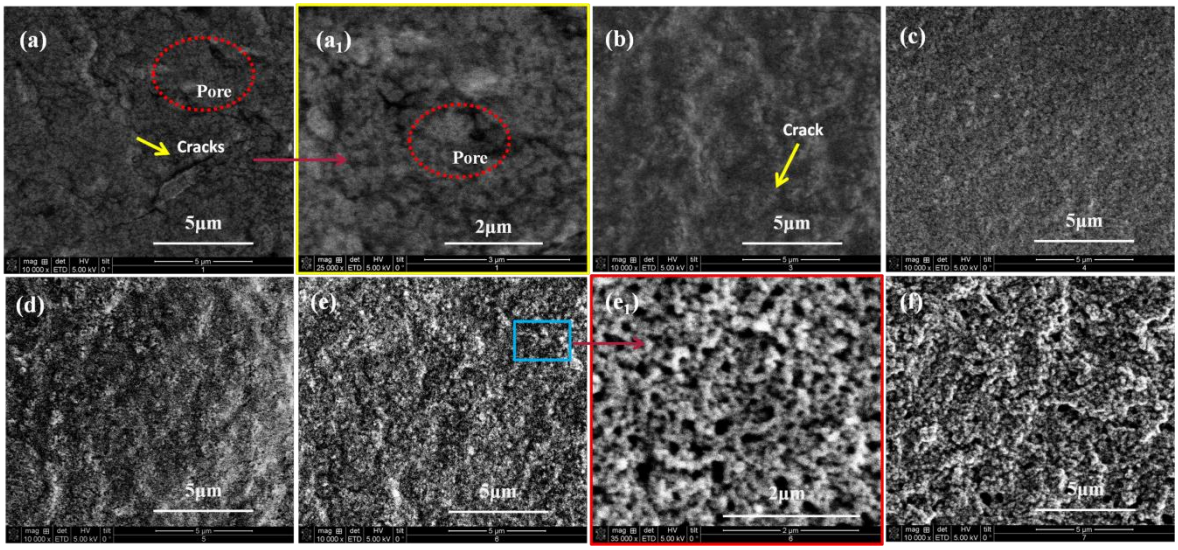

Fig.9. SEM images of silver films sintered for 60 minutes, (a) 125°C, (b) 140°C, (c) 155°C, (d) 170°C, (e) 185°C and (f) 200°C (a_1 and e_1 are high magnification images of a and e)

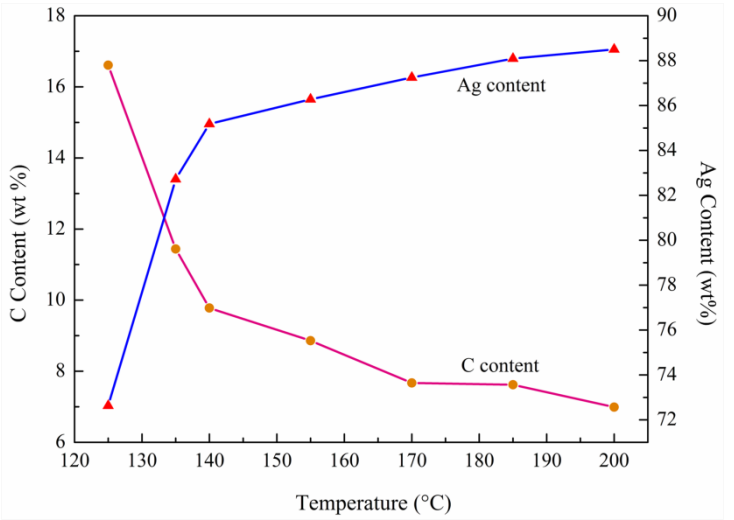

Fig.10. C and Ag content from EDX results in the films as a function of sintering temperature

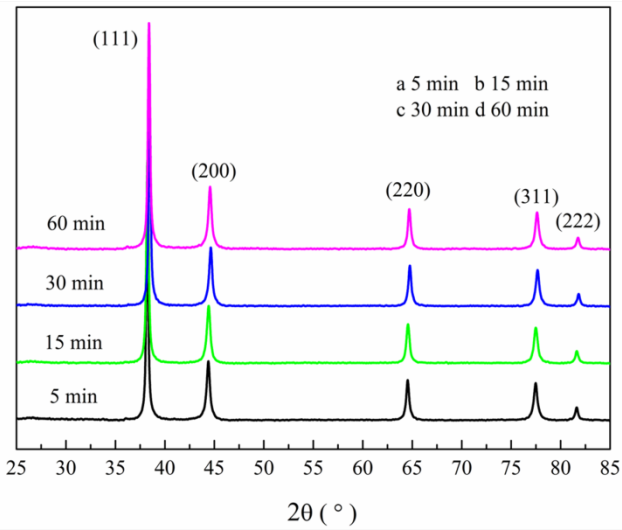

Fig.11. XRD patterns of Ag films prepared at 155°C for 5, 15, 30 and 60 min respectively

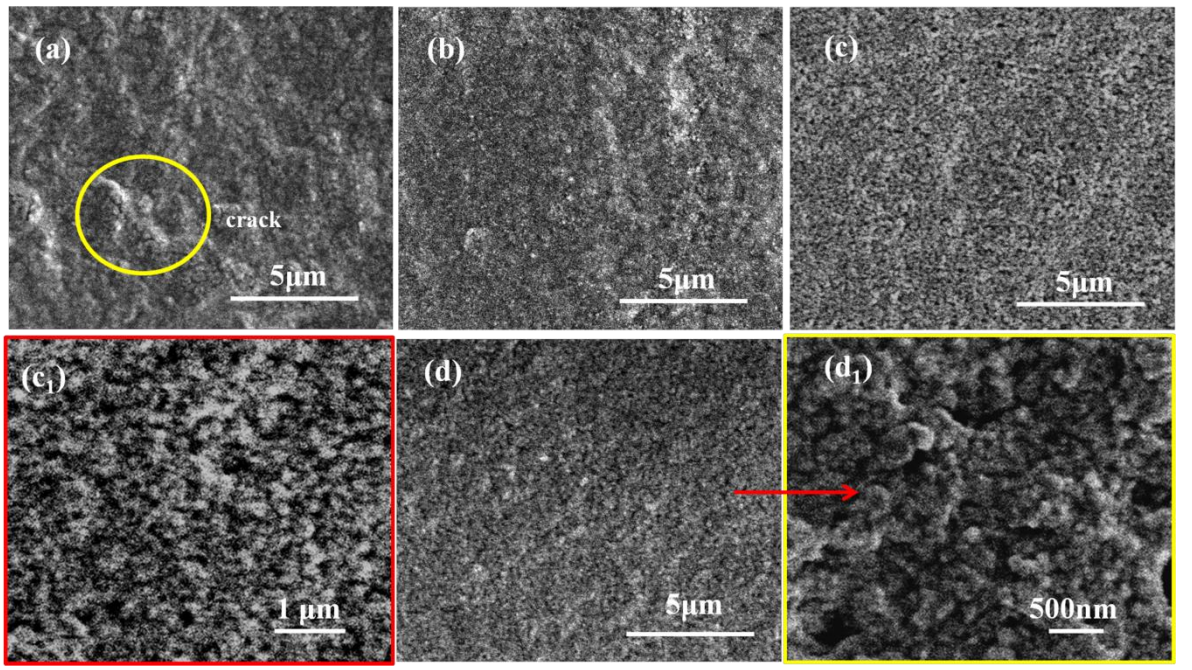

Fig.12. SEM images of silver films produced at 155 °C for 5, 15, 30 and 60 minutes (a-d, c_1 and d_1 are high magnification image of c and d)

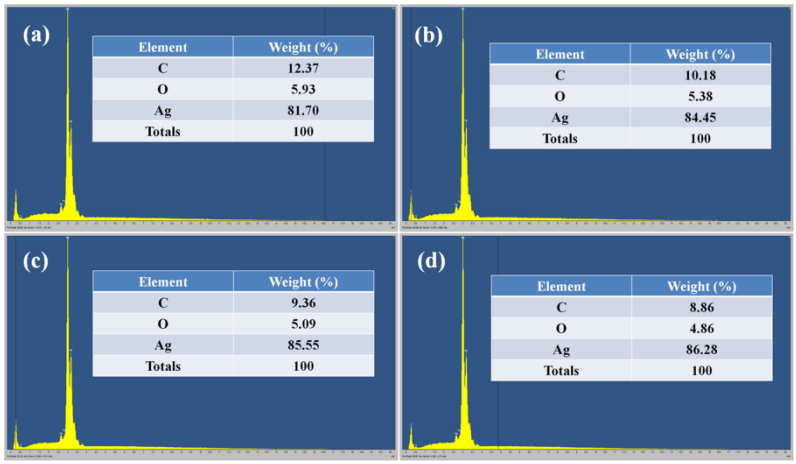

Fig.13. EDX results of silver films produced at 155°C for 5, 15, 30 and 60 minutes (a-d)

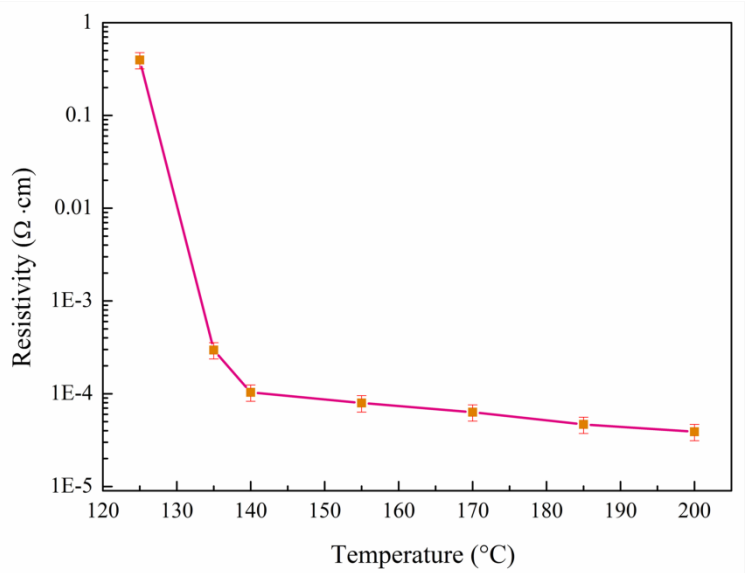

Fig.14. Resistivity of the silver films sintered at various temperatures for 60 minutes

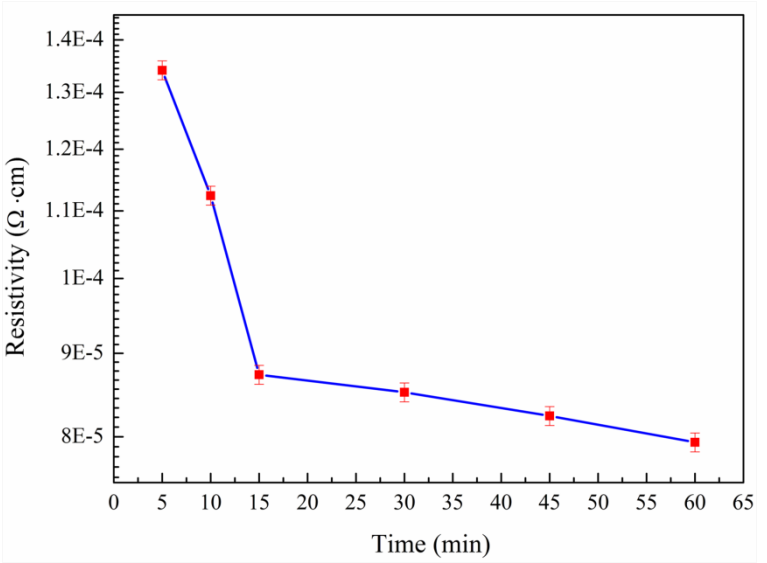

Fig.15. Resistivity of the Ag films as a function of heating time at 155°C

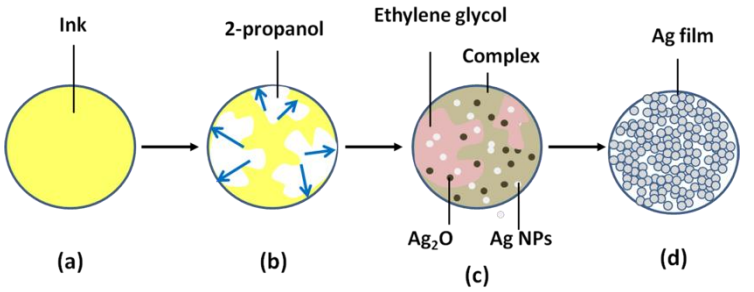

Fig.16. Schematic illustration for the film formation process of the silver ink